RSC Advances

PAPER

View Article Online
View Journal | View Issue

Cite this: RSC Adv., 2017, 7, 1841

Fluorescence of ZnO/carbon mixture and application in acid rain detection†

Kai-Kai Liu,[ab] Chong-Xin Shan,*[ac] Hong-Zhen Liu,[ab] Qing Lou[c] and De-Zhen Shen*[a]

Received 9th November 2016
Accepted 13th December 2016

DOI: 10.1039/c6ra26523e

www.rsc.org/advances

A ZnO and carbon nanoparticle (NP) mixture has been prepared. The fluorescence color of the mixture changes from yellow to blue when the pH value of the ambient is smaller than 5.5, which accords well with the pH standard value of acid rain (<5.6). This colorimetric change can be observed clearly by the naked eye, and thus the mixture can be employed as a probe to detect acid rain. The mechanism for the colorimetric change can be attributed to the fluorescence quenching of the ZnO NPs in acidic conditions. The results demonstrated in this paper provide a visual detection route for acid rain by the naked eye for the first time, and thus may be promising for the wide application of acid rain detection in the future.

1 Introduction

Fluorescent nanoparticles (NPs) including metal oxide NPs,[1–3] rare earth NPs,[4–7] carbon NPs,[8–11] and polymer NPs[12,13] have attracted much attention in recent years due to their unique optical and electrical properties. Among these NPs, ZnO and carbon NPs have been highlighted for their low toxicity and eco-friendly characters.[14–16] Carbon and ZnO NPs share some unique characters like excellent luminescent property, good photo-bleaching resistance, and mild synthesis conditions. Because of the above characteristics, ZnO and carbon NPs have potential applications in many fields including labeling, light-emitting devices, bioimaging, drug delivery, *etc.* Acid rain refers to the deposition of a mixture from wet and dry acidic components, whose pH value is lower than 5.6. Generally, acid rain is mainly caused by the emissions of sulfur dioxide (SO_2) and nitrogen oxides (NO and NO_2), both of which react with water molecules in the atmosphere to produce acid rain. SO_2 and NO_2 can dissolve easily in water and form a pH-dependent equilibrium mixture with sulfite, bisulfite and nitrate anions. Acid rain, as an environmental issue, has huge adverse impact on forests, lakes, and soils, may lead to the death of insects and aquatic life-forms, and also may cause severe corrosion of buildings and steel products.[17–21] There are quite a few reports on the detection of SO_2 (ref. 22–27) and NO_2 (ref. 28–30) and derivatives,[31–43] which are the essential components in acid rain, through colorimetric, fluorescent and optical methods. In general, for ions with low concentration recognition is more difficult in aqueous media because of the strong solvation effect,[44] which often requires troublesome sample pre-treatment, and time-consuming and complicated instrumentation to determine acid rain.

In this paper, a ZnO and carbon NP mixture is used as dual-emission ratiometric fluorescent sensor to detect acid rain. In this system, fluorescence of the ZnO and carbon NP mixture can be influenced greatly by the pH value of the ambient. The color of the mixture changes from yellow to blue when the pH value is smaller than 5.5, which accords well with the standard pH value of acid rain (<5.6). Moreover, the carbon NPs in this system are used for a reference signal, so that it is easy to judge whether the variation in fluorescence intensity is due to induced changes or from misoperations, or other instrumental problems. Thus a route to determine acid rain by the naked eye based on the variation in fluorescence of the ZnO and carbon NP mixture has been demonstrated for the first time. The mechanism for the color change of the mixture can be attributed to the fluorescence quenching of the ZnO NPs in acidic ambient, while that of the carbon NPs is almost independent of the pH value of the sampling solution.

2 Experimental section

2.1 Materials

The reagents used in our experiments were zinc acetate dihydrate ($Zn(Ac)_2 \cdot 2H_2O$), (3-aminopropyl)triethoxysilane (APTES), potassium hydroxide (KOH), citric acid, and ethylenediamine. The chemical reagents were of analytical grade and used without further purification.

2.2 Synthesis of ZnO NPs

The preparation procedure of ZnO NPs was as follows: 5.5 g (25 mmol) $Zn(Ac)_2 \cdot 2H_2O$ was dissolved in 150 ml ethanol solution, and the solution was refluxed at 80 °C for 2 hours under

[a]State Key Laboratory of Luminescence and Applications, Changchun Institute of Optics, Fine Mechanics and Physics, Chinese Academy of Sciences, Changchun 130033, China. E-mail: shendz@ciomp.ac.cn
[b]University of Chinese Academy of Sciences, Beijing 100049, China
[c]School of Physics and Engineering, Zhengzhou University, Zhengzhou 450001, China

† Electronic supplementary information (ESI) available. See DOI: 10.1039/c6ra26523e

continuous stirring until it formed a transparent solution. Then 20 ml 1.75 M KOH ethanol solution was added into the $Zn(Ac)_2 \cdot 2H_2O$ ethanol solution under continuous stirring at 0 °C until it became colorless and transparent. Finally, 1.5 ml deionized water and 400 μl (3-(2,3-epoxypropoxy)propyl)trimethoxysilane were added into the ZnO NP solution until it became turbid. After that, the solution was centrifuged (6000 rpm, 10 min) and the obtained precipitates were washed using water several times to remove the unreacted precursors. The washed precipitate was then placed into an oven (75 °C) for 12 hours for further applications.

2.3 Synthesis of carbon NPs

0.42 g citric acid and 536 μl ethylenediamine were dissolved in 10 ml deionized water. Then the solution was transferred to an autoclave and heated at 200 °C for 5 h. After that, the reaction was cooled to room temperature naturally. The product was centrifuged (5000 rpm, 20 min) in order to obtain the carbon NPs and the resulting solution was stored under normal conditions for further applications.

2.4 Preparation of ZnO and carbon NP mixture

The preparation procedure of carbon/ZnO NP mixed solution was as follows: 1 ml as-prepared carbon NP aqueous solution was diluted to 10 ml with deionized water, and then the diluted carbon NP aqueous solution was mixed with ZnO NP aqueous solution (10 mg ml^{-1}) with a volume ratio of 1 : 4000 to prepare carbon/ZnO NP mixed solution.

2.5 Printing of carbon/ZnO NP mixture solution

The as-prepared carbon/ZnO mixed solution was injected into the cartridge of a printer (HP-1510) as ink. Then the cartridge was put into the printer, and the ink was printed onto a non-fluorescent paper by the printer to form patterns.

2.6 Characterizations

The structural properties of the ZnO and carbon NPs were characterized by using a JEM-2010 transmission electron microscope. The fluorescence properties of the NPs were determined with a HITACHI F-7000 spectrophotometer. The absorption spectra of the samples were measured with a Shimadzu UV-3101PC spectrometer. Fluorescence quantum yields of the samples were obtained with a calibrated integrating sphere in a FLS920 spectrometer.

3 Results and discussion

3.1 Structural characterizations

The morphological and structural properties of the ZnO and carbon NPs used in this paper have been characterized carefully, as shown in Fig. 1. Fig. 1(a) and (d) show clearly that both the ZnO and carbon NPs are spherical in shape. Clear lattice fringes can be observed from the high-resolution TEM images of both kinds of NPs, and the spacing between the adjacent fringes of the ZnO and carbon NPs is about 0.26 nm and 0.21 nm, respectively, which reveals the good crystalline nature of the NPs, as shown in Fig. 1(b) and (e). One droplet each of ZnO and carbon NP solutions was dropped upon a piece of glass slide, and the ZnO droplet shows bright yellowish fluorescence, while the carbon droplet shows blue emission under UV illumination, as indicated in Fig. 1(c) and (f). The elements of ZnO and carbon mixture were investigated by XPS analysis (Fig. 1(g)). The peaks for C 1s, N 1s, O 1s, Zn 2p and Si 2p have been marked in Fig. 1(g), indicating ZnO and carbon NPs can co-exist in this system without mutual disruption. The XPS patterns of N 1s, O 1s, Zn 2p and Si 2p are shown in Fig. S1.† The elemental content of ZnO and carbon NP mixture is listed in Table S1.† Fourier transform infrared (FTIR) spectra of the ZnO NPs have been recorded by the KBr method, as shown in Fig. S2.† The stretching vibration bands of N–H and O–H (3000–3500 cm^{-1}) can be observed clearly, indicating that the NPs can be dispersed well in aqueous solution owing to the existence of these hydrophilic functional groups. C 1s XPS analysis displays three different peaks, which represent three different carbon atoms (graphitic and aliphatic carbon, oxygenated carbon, nitrous carbon),[45] as shown in Fig. 1(h). Moreover, the crystalline properties of ZnO and carbon NPs were characterized by X-ray diffraction (XRD), as shown in Fig. S3.† In Fig. S3(a),† some broad diffraction peaks can be observed, which are attributed to the diffraction from wurtzite ZnO (JCPDS 89-1397). The XRD pattern of carbon NPs shown in Fig. S3(b)† displays a broad peak centered at around 25°, which can be attributed to highly discorded carbon atoms.[46]

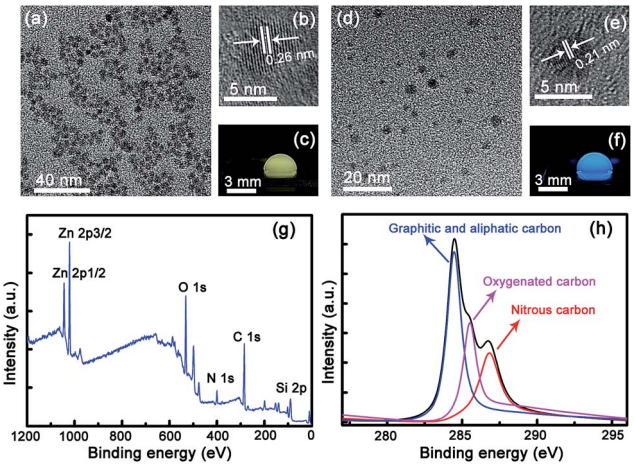

Fig. 1 (a) TEM image of the ZnO NPs. (b) High-resolution TEM image of the ZnO NPs. (c) Fluorescence image of a droplet of the ZnO NP solution. (d) TEM image of the carbon NPs. (e) High-resolution TEM image of the carbon NPs. (f) Fluorescence image of a droplet of the carbon NP solution. (g) XPS of ZnO and carbon NP mixture. (h) C 1s patterns.

3.2 Optical properties of ZnO and carbon NPs

The fluorescence spectra of the ZnO NPs with concentration ranging from 5 mg ml^{-1} to 15 mg ml^{-1} have been measured, as shown in Fig. 2(a). All the spectra are dominated by a broad emission at around 580 nm, which can be attributed to the deep-level emission of ZnO.[47–49] The fluorescence intensity

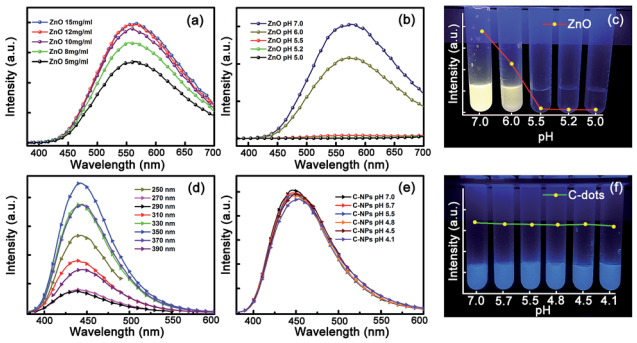

Fig. 2 (a) The fluorescence spectra of the ZnO NP solution with concentrations ranging from 5 to 15 mg ml^{-1}. (b) The fluorescence spectra of the ZnO NP solution at different pH values. (c) The fluorescence images and intensity of the ZnO NP solution at different pH values. (d) The fluorescence spectra of the carbon NP solution for varying excitation wavelengths. (e) The fluorescence spectra of the carbon NP solution at different pH values. (f) The fluorescence images and intensity of the carbon NP solution at different pH values.

increases gradually with concentration in the investigated range, but when the concentration is increased further, the fluorescence intensity tends to saturate; thus ZnO NP solution with a concentration of 10 mg ml^{-1} has been employed as an example in the following investigations. The typical absorption spectra of the ZnO NPs have been measured (see Fig. S4†), and all the spectra show a strong absorption in the wavelength region shorter than 400 nm, while it is almost negligible in the visible region. Fig. 2(b) shows the fluorescence spectra of the ZnO NPs in solution with different pH values. It is seen that the fluorescence intensity decreases with the decreasing of the pH value of the sampling solution, and when the pH value is smaller than 5.5, the fluorescence of the ZnO NPs almost vanishes completely. This phenomenon can also be observed clearly from the fluorescence image and intensity of the ZnO NP solution shown in Fig. 2(c). These results reveal that the fluorescence of the ZnO NPs is very sensitive to the pH value at ambient. To investigate the fluorescence quenching mechanism in acidic ambient of the ZnO NPs, the absorption spectra of the ZnO NP solution with different pH values have been measured (see Fig. S5†). The strong absorption at wavelengths shorter than 400 nm almost disappears in acidic conditions, indicating that the fluorescence quenching of the ZnO NPs is mainly owing to the decomposition of ZnO.

The fluorescence spectra of the carbon NPs under different excitation wavelengths have been recorded (Fig. 2(d)). The strongest emission centered at 450 nm is observed under the excitation of a UV lamp, with a fluorescence quantum yield of around 60%. To study the fluorescence properties of the carbon NPs in acidic condition, the fluorescence spectra of the carbon NP solution with different pH values have also been measured, as shown in Fig. 2(e). The fluorescence intensity of the carbon NPs remains almost unchanged with the pH decreasing from 7.0 to 4.1, indicating that the carbon NPs can be used for a reference signal in acid rain detection. The absorption spectra of carbon NPs with different pH values were also measured, as shown in Fig. S6.† The absorption spectra show little change with different pH conditions, revealing that the carbon NPs cannot be affected much by the pH value of the solution in our investigation range. The fluorescence images and intensity of the carbon NPs with different pH values are shown in Fig. 2(f). It can be seen that the fluorescence color and intensity show little change visually, which matches well with the fluorescence spectra.

3.3 pH sensing of ZnO and carbon NP mixture

The ZnO and carbon NP mixture is thus used as a dual-emission ratiometric fluorescent pH sensor based on the above results. The fluorescence spectra of the ZnO and carbon NP mixed solution with different pH values under excitation at a wavelength of 254 nm are shown in Fig. 3(a). The spectrum of the mixed solution with pH of 7.0 shows a dominant broad emission at around 580 nm, while that of the mixed solution with pH value of 5.5 shows a band located at around 450 nm. The fluorescence spectra of ZnO and carbon NP mixed solution with different pH values under excitation at a wavelength of 365 nm are also recorded in Fig. S7(a).† Two peaks centered at around 450 nm and 580 nm can be observed clearly, while the peaks centered at around 580 nm diminish gradually when the pH value of solution decreases. The corresponding color coordinates are also shown in Fig. S7(b).† In view of colorimetric sensitivity of the eyes, a UV lamp with 254 nm line is the better choice. The results indicate that the color has changed from yellow to blue when the pH value of this mixed solution decreases from 7.0 to 5.5, which is verified by the fluorescence images of the mixed solution shown in the inset of Fig. 3(a). The absorption spectra of the ZnO and carbon NP mixed solution were measured and are shown in Fig. 3(b). The absorption spectrum of the mixture shares the same lineshape as the absorption spectrum of the ZnO NPs

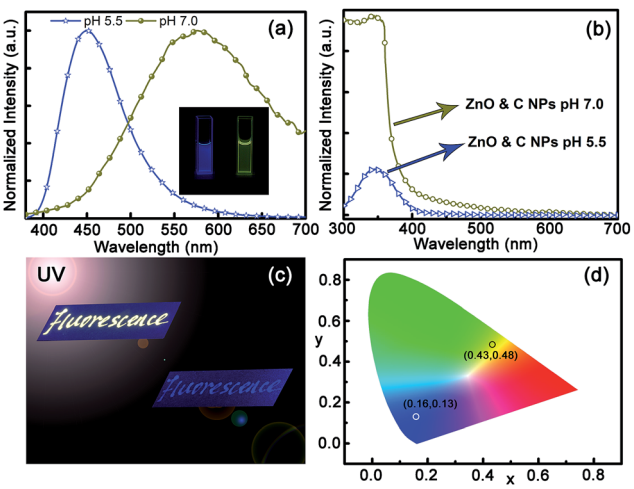

Fig. 3 (a) The fluorescence spectra of the ZnO and carbon NP mixed solution with different pH values under excitation with the 254 nm line of a xenon lamp; the inset shows the corresponding fluorescence image. (b) The absorption spectra of the ZnO and carbon mixed solution with pH of 7.0 and 5.5. (c) The characters of "fluorescence" written on copy paper using ZnO and carbon NP mixed solution as ink in neutral ambient and acidic ambient under illumination of the 254 nm line of a UV lamp. (d) The corresponding color coordinates of the characters in neutral and acidic ambient.

shown in Fig. S4† when the pH value of the mixed solution is 7.0, while it shares the same lineshape as that of carbon NPs shown in Fig. S6† when the pH value of the mixed solution is 5.5, indicating that ZnO NPs have been decomposed while carbon NPs remain in acidic condition. The word "fluorescence" was written on copy paper by employing the mixed solution as ink, and the characters can be observed clearly under illumination of the 254 nm line of a UV lamp, as indicated in Fig. 3(c). The characters show yellow fluorescence under neutral ambient, and the color coordinate is (0.43, 0.48), while the color changes to blue when the paper is placed in acidic ambient within several seconds, with the color coordinate changing to (0.16, 0.13), as indicated in Fig. 3(d). The above data indicate that the color of the mixed solution can be employed as a colorimetry probe of acidic ambient by the naked eye.

3.4 Application for detection of simulated acid rain

Since acid rain is moisture containing mainly SO_2 and NO_2 gases, to confirm the applicability of such a route in determining acid rain, an image has been printed by employing ZnO and carbon NP mixed solution as ink, as shown in Fig. 4(a). The upper area of the printed image is exposed to atmosphere with SO_2- and NO_2-containing moisture for several seconds, while the lower area is shielded by a mask. The fluorescence color of the lower part of the printed image keeps almost unchanged, while that of the upper part has transformed from yellow to blue, as indicated in Fig. 4(b). For clarity, the image shown in Fig. 4(b) has been extracted through blue and yellow channels, as shown, respectively, in Fig. 4(c) and (d). The images in Fig. 4(c) and (d) have been merged into a single image, as shown in Fig. 4(e). Both the blue logo and yellow characters can be observed clearly,

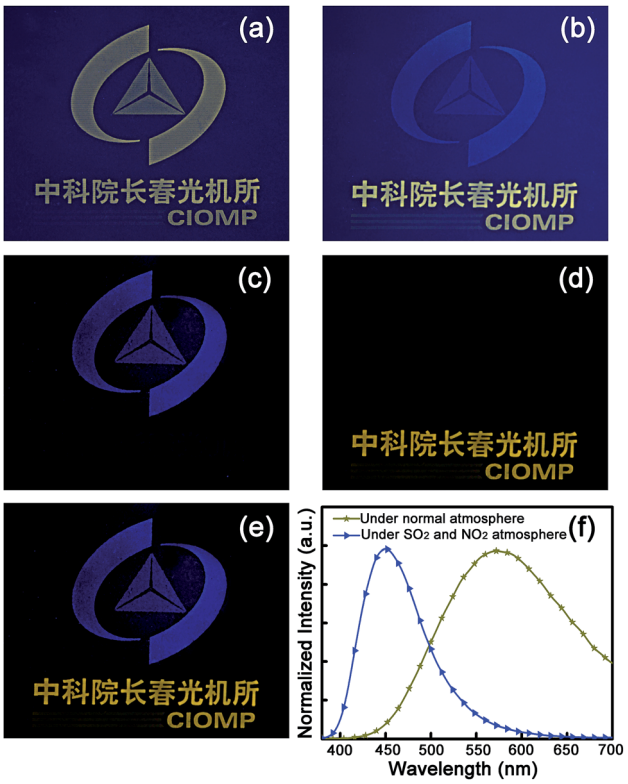

Fig. 4 (a) Photograph of a printed image using the ZnO and carbon NP mixed solution as ink under UV illumination. (b) Photograph of the printed image with upper part exposed to SO_2 and NO_2 gases for several seconds. (c) The image extracted from (b) through a blue channel and (d) the image extracted from (b) through a yellow channel. (e) The merged image of (c) and (d). (f) The fluorescence spectra of the printed image under neutral and SO_2 and NO_2 gas atmospheres under UV illumination.

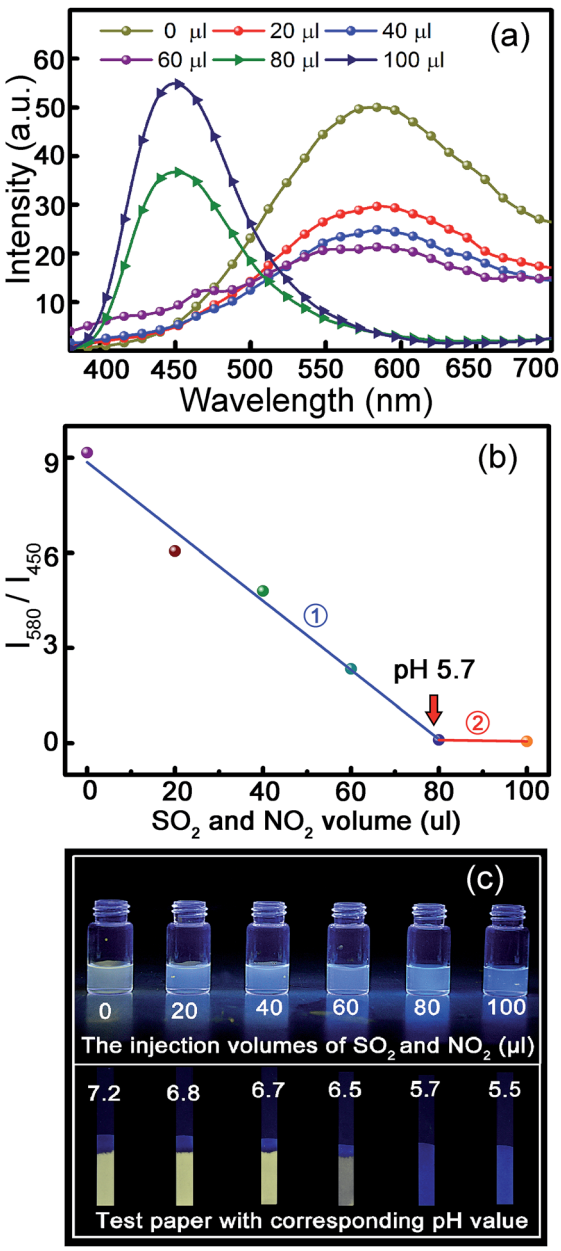

Fig. 5 (a) Fluorescence spectra of the ZnO and carbon NP mixed solution with different injection volumes of SO_2 and NO_2 gases. (b) Ratiometric curve between I_{580} and I_{450} *versus* SO_2 and NO_2 gas mixture volume. (c) The fluorescent images of paper slips immersed in the ZnO and carbon NP mixed solution with different injection volumes of SO_2 and NO_2 gases; the pH value of the solution after the gas injection is indicated.

indicating the feasibility of this method for detection of acid rain. The fluorescence spectra of the printed image under neutral and SO_2 and NO_2 gas atmospheres are shown in Fig. 4(f). It is evident that the image shows a dominant emission band at around 580 nm under neutral ambient, which corresponds to the fluorescence of ZnO NPs, while the spectrum is dominated by an emission centered at around 450 nm under acidic ambient, which corresponds to the fluorescence of carbon NPs.

As mentioned above, the major ingredients of acid rain are SO_2 and NO_2, and its pH is lower than 5.6. SO_2 and NO_2 gas mixture with different volumes was hence injected into a ZnO and carbon NP mixed solution (2 ml), and the fluorescence spectra of the mixed solution are shown in Fig. 5(a). It is evident that the fluorescence spectrum of the ZnO and carbon NP mixed solution without SO_2 and NO_2 shows a broad emission at around 580 nm under UV illumination. The fluorescence intensity decreases gradually with the volume of SO_2 and NO_2 gases increasing from 20 to 60 μl, while only a broad emission at around 450 nm can be observed when the volume of SO_2 and NO_2 gases reaches 80 μl. The fluorescence intensities of peaks centered at 580 nm and 450 nm are denoted as I_{580} and I_{450}, and the ratio between I_{580} and I_{450} *versus* volume of SO_2 and NO_2 mixture is shown in Fig. 5(b). The scatter points are divided into two groups, which are processed by linear fitting, respectively. The slopes of the two fitting lines are −0.109 and −0.002. The joint point of straight lines 1 and 2 is the saltation point of the slope, indicating the pH has dropped to below 5.7 (marked with red arrow). The fluorescence images of the ZnO and carbon NP mixed solution, in which the injected volumes of SO_2 and NO_2 gas mixture are successively 0, 20, 40, 60, 80, and 100 μl, are shown in the upper part of Fig. 5(c). The pH values of the mixed solution after the injection of the gas have been recorded, as indicated in the lower part of Fig. 5(c). Also, paper slips have been dipped into the solution, and images of the paper slips under UV illumination are shown in the lower part of Fig. 5(c). The slips show bright yellow color without injection of SO_2 and NO_2 gases, while the yellow color weakens with the increase of the gas volume, and the color of the paper slips changes to blue when the injection gas volume is larger than 80 μl (corresponding to a pH value of 5.7, in good accord with the pH standard of acid rain of 5.6), which promises applicability of such a route in probing acid rain by the naked eye, avoiding the utilization of complicated scientific instruments, and thus may give impetus to the wide applications of acid rain determination.

Acknowledgements

This work is financially supported by the National Science Foundation for Distinguished Young Scholars of China (61425021), the Natural Science Foundation of China (11374296, 61376054, and 61475153), and the National Program for Support of Top-notch Young Professionals.

Notes and references

1 X. Tang, E. S. G. Choo, L. Li, J. Ding and J. Xue, *Chem. Mater.*, 2010, **22**, 3383–3388.
2 X. Wang, X. Kong, Y. Yu and H. Zhang, *J. Phys. Chem. C*, 2007, **111**, 3836–3841.
3 Z. Y. Zhang, Y. D. Xu, Y. Y. Ma, L. L. Qiu, Y. Wang, J. L. Kong and H. M. Xiong, *Angew. Chem., Int. Ed.*, 2013, **52**, 4127–4131.
4 Q. Liu, M. Chen, Y. Sun, G. Chen, T. Yang, Y. Gao, X. Zhang and F. Li, *Biomaterials*, 2011, **32**, 8243–8253.
5 H.-P. Zhou, C.-H. Xu, W. Sun and C.-H. Yan, *Adv. Funct. Mater.*, 2009, **19**, 3892–3900.
6 L. Li, K. Green, H. Hallen and S. F. Lim, *Nanotechnology*, 2015, **26**, 025101.
7 X. Zhao, S. He and M. C. Tan, *J. Mater. Chem. C*, 2016, **4**, 8349–8372.
8 Ya.-P. Sun, X. Wang, F. Lu, L. Cao, M. J. Meziani, P. G. Luo, L. Gu and L. M. Veca, *J. Phys. Chem. C*, 2008, **112**, 18295–18298.
9 D. Qu, M. Zheng, J. Li, Z. Xie and Z. Sun, *Light: Sci. Appl.*, 2015, **4**, e364.
10 K. Ku, S. W. Lee, J. Park, N. Kim, H. Chung, C. H. Han and W. Kim, *Nanotechnology*, 2014, **25**, 395601.
11 Y. Liu, P. Wang, K. A. Shiral Fernando, G. E. LeCroy, H. Maimaiti, B. A. Harruff-Miller, W. K. Lewis, C. E. Bunker, Z.-L. Hou and Y.-P. Sun, *J. Mater. Chem. C*, 2016, **4**, 6967–6974.
12 A. Topete, M. Alatorre-Meda, P. Iglesias, E. M. Villar-Alvarez, S. Barbosa, J. A. Costoya, P. Taboada and V. c. Mosquera, *ACS Nano*, 2014, **8**, 2725–2738.
13 A. Reisch and A. S. Klymchenko, *Small*, 2016, **12**, 1968–1992.
14 Q. Lou, S. Qu, P. Jing, W. Ji, D. Li, J. Cao, H. Zhang, L. Liu, J. Zhao and D. Shen, *Adv. Mater.*, 2015, **27**, 1389–1394.
15 S. Y. Fu, X. W. Du, S. A. Kulinich, J. S. Qiu, W. J. Qin, R. Li, J. Sun and J. Liu, *J. Am. Chem. Soc.*, 2007, **129**, 16029–16033.
16 X. Wang, S. Zhou and L. Wu, *J. Mater. Chem. C*, 2013, **1**, 7547.
17 J. Chen, W. Li and F. Gao, *J. Environ. Monit.*, 2010, **12**, 1799–1806.
18 G. E. Likens, C. T. Driscoll and D. C. Buso, *Science*, 1996, **272**, 244–246.
19 F. Rosso, W. Jin, A. L. Pisello, M. Ferrero and M. Ghandehari, *Construct. Build. Mater.*, 2016, **108**, 146–153.
20 V. Velikova, I. Yordanov and A. Edreva, *Plant Sci.*, 2000, **151**, 59–66.
21 X. Zhang, L. Wang, A. Zhou, Q. Zhou and X. Huang, *Ecotoxicol. Environ. Saf.*, 2016, **126**, 62–70.
22 H. Li, H. Zhu, M. Sun, Y. Yan, K. Zhang, D. Huang and S. Wang, *Langmuir*, 2015, **31**, 8667–8671.
23 M. Sun, H. Yu, K. Zhang, Y. Zhang, Y. Yan, D. Huang and S. Wang, *Anal. Chem.*, 2014, **86**, 9381–9385.
24 M. Albrecht, R. A. Gossage, M. Lutz, A. L. Spek and G. v. Koten, *Chem.–Eur. J.*, 2000, **6**, 1431–1445.
25 A. V. Leontiev and D. M. Rudkevich, *J. Am. Chem. Soc.*, 2005, **127**, 14126–14127.
26 A. Farooq, R. Al-Jowder, R. Narayanaswamy, M. Azzawi, P. J. R. Roche and D. E. Whitehead, *Sens. Actuators, B*, 2013, **183**, 230–238.
27 K. Wu, J. Guo and C. Wang, *Chem. Commun.*, 2014, **50**, 695–697.
28 L. Li, C. Zhang and W. Chen, *Nanoscale*, 2015, **7**, 12133–12142.
29 A. Gulino, T. Gupta, P. G. Mineo and M. E. van der Boom, *Chem. Commun.*, 2007, 4878.

30 C. W. Na, H. S. Woo, I. D. Kim and J. H. Lee, *Chem. Commun.*, 2011, **47**, 5148–5150.
31 W. Chen, Q. Fang, D. Yang, H. Zhang, X. Song and J. Foley, *Anal. Chem.*, 2015, **87**, 609–616.
32 S. Chen, P. Hou, J. Wang and X. Song, *RSC Adv.*, 2012, **2**, 10869.
33 X. Cheng, H. Jia, J. Feng, J. Qin and Z. Li, *Sens. Actuators, B*, 2013, **184**, 274–280.
34 Y. Sun, S. Fan, S. Zhang, D. Zhao, L. Duan and R. Li, *Sens. Actuators, B*, 2014, **193**, 173–177.
35 Y. Sun, D. Zhao, S. Fan, L. Duan and R. Li, *J. Agric. Food Chem.*, 2014, **62**, 3405–3409.
36 Y. Q. Sun, J. Liu, J. Zhang, T. Yang and W. Guo, *Chem. Commun.*, 2013, **49**, 2637–2639.
37 G. Wang, H. Qi and X. F. Yang, *Luminescence*, 2013, **28**, 97–101.
38 M. Y. Wu, T. He, K. Li, M. B. Wu, Z. Huang and X. Q. Yu, *Analyst*, 2013, **138**, 3018–3025.
39 M. Y. Wu, K. Li, C. Y. Li, J. T. Hou and X. Q. Yu, *Chem. Commun.*, 2014, **50**, 183–185.
40 H. Xie, F. Zeng, C. Yu and S. Wu, *Polym. Chem.*, 2013, **4**, 5416.
41 X.-F. Yang, M. Zhao and G. Wang, *Sens. Actuators, B*, 2011, **152**, 8–13.
42 Y. Yang, F. Huo, J. Zhang, Z. Xie, J. Chao, C. Yin, H. Tong, D. Liu, S. Jin, F. Cheng and X. Yan, *Sens. Actuators, B*, 2012, **166–167**, 665–670.
43 D. Liu, Z. Wang and X. Jiang, *Nanoscale*, 2011, **3**, 1421–1433.
44 E. J. O'Neil and B. D. Smith, *Coord. Chem. Rev.*, 2006, **250**, 3068–3080.
45 S. Zhu, Q. Meng, L. Wang, J. Zhang, Y. Song, H. Jin, K. Zhang, H. Sun, H. Wang and B. Yang, *Angew. Chem., Int. Ed.*, 2013, **52**, 3953–3957.
46 S. Qu, X. Wang, Q. Lu, X. Liu and L. Wang, *Angew. Chem., Int. Ed.*, 2012, **51**, 12215–12218.
47 H.-M. Xiong, Y. Xu, Q.-G. Ren and Y.-Y. Xia, *J. Am. Chem. Soc.*, 2008, **130**, 7522–7523.
48 L. Zhang, L. Yin, C. Wang, N. lun, Y. Qi and D. Xiang, *J. Phys. Chem. C*, 2010, **114**, 9651–9658.
49 M. Dutta, S. Jana and D. Basak, *ChemPhysChem*, 2010, **11**, 1774–1779.